Interaction and Multiscale Mechanics, Vol. 3, No. 1 (2010) 39-54
DOI: http://dx.doi.org/10.12989/imm.2010.3.1.039

The influence of different support movements and heights of piers on the dynamic behavior of bridges. Part II: earthquake acting along the bridge axis

I.G. Raftoyiannis, T.G. Konstantakopoulos and G.T. Michaltsos*

Laboratory of Steel Structures, Department of Civil Engineering,
National Technical University of Athens,
9 Iroon Polytechneiou St., Zografou Campus, Athens 15780, Greece

(Received September 14, 2009, Accepted January 19, 2010)

Abstract. In this paper, a simple approach is presented for studying the dynamic response of multi-span steel bridges supported by pylons of different heights, subjected to earthquake motions acting along the axis of the bridge with spatial variations. The analysis is carried out using the modal analysis technique, while the solution of the integral-differential equations derived is obtained using the successive approximations technique. It was found that the height of piers and the quality of the foundation soil can affect significantly the dynamical behavior of the bridges studied. Illustrative examples are presented to highlight the points of concern and useful conclusions are gathered.

Keywords: bridge dynamics; piers; earthquakes; axial motion.

1. Introduction

Strong earthquake motion is a phenomenon occasionally encountered in seismic-prone regions. For structures that are really long, the spatial variability of strong earthquake motion over small distance may have to be considered. This variation in the temporal and frequency characteristics of ground motions may produce forces in long-span structures that are absent in structures with uniform excitations.

Factors for spatial variation of ground motions include: the absence of homogeneity of the ground material, the nature of the propagating waves of the seismic excitation leading to different arrival times at the supports, the decay of wave amplitudes within small distances due to a possibly existing fault or due to geometric and material energy dissipation, and variable ground conditions leading to different surface motions along the structure. As far as bridges are concerned, the effect of non-uniform seismic excitations on the response of the structure has been studied extensively for more than two decades. Research along these lines includes the works of Bogdanoff *et al*. (1965), Harichandran and Wang (1990), Zerva (1990), Abrahamson *et al*. (1991), Betti *et al*. (1993), Monti

* Professor, Corresponding author, E-mail: michalts@central.ntua.gr

et al. (1996), Price and Eberhard (1998), and Nikolaou *et al*. (2001). As suggested by Part 2 of Eurocode 8 for bridges (2002), the influence of the pylon's height on the bridge-deck dynamic behavior should be taken into account without any further comments or instructions.

In a companion paper, the effect of earthquakes acting transversely to the axis of bridges resting on piers of different heights and support conditions has been thoroughly studied using a simple analytical model. In this paper, concerning the wave propagation and soil structure interaction effects, a simple model is developed for analyzing the response of long bridges resting on tall or short pylons and subjected to spatially varying ground motions. The structural system considered, where shear deformation is neglected, can be analyzed as a bridge-deck continuous beam (with known eigenshapes U_n, X_n and eigenfrequencies ω_n), supported by pylons represented by cantilever beams (with also known eigenshapes $\overline{X}_n$ and eigenfrequencies $\overline{\omega}_n$).

Using the "influence functions" $g(x)$ of the bridge-deck (that express the deformation of a beam due to unit displacement of its supports), along with the modal analysis technique, and the compatibility conditions at the supports, we can derive the integral-differential equations of the system as functions of time and joints motions. The aforementioned equations are solved by the successive approximations method. The resulting expressions are calculated numerically using the Mathematica symbolic manipulator. Illustrative examples are given to show the effectiveness and reliability of the method, and useful conclusions are drawn.

2. Basic assumptions

The following assumptions are adopted in the present analysis:

a. The bridge, shown in Fig. 1, is resting on a number of pylons that are either fixed or hinged to the ground. We assume that each pylon has a different displacement at its base and that for the i^{th} pylon such a displacement is denoted as $f_i(t)$.

b. The axial and shear deformations of the pylons are neglected.

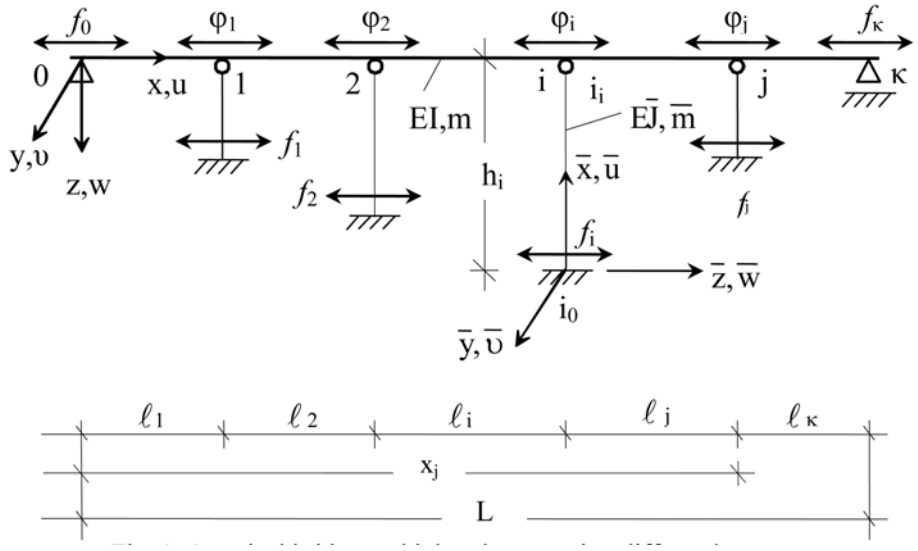

Fig. 1 A typical bridge on high pylons moving differently

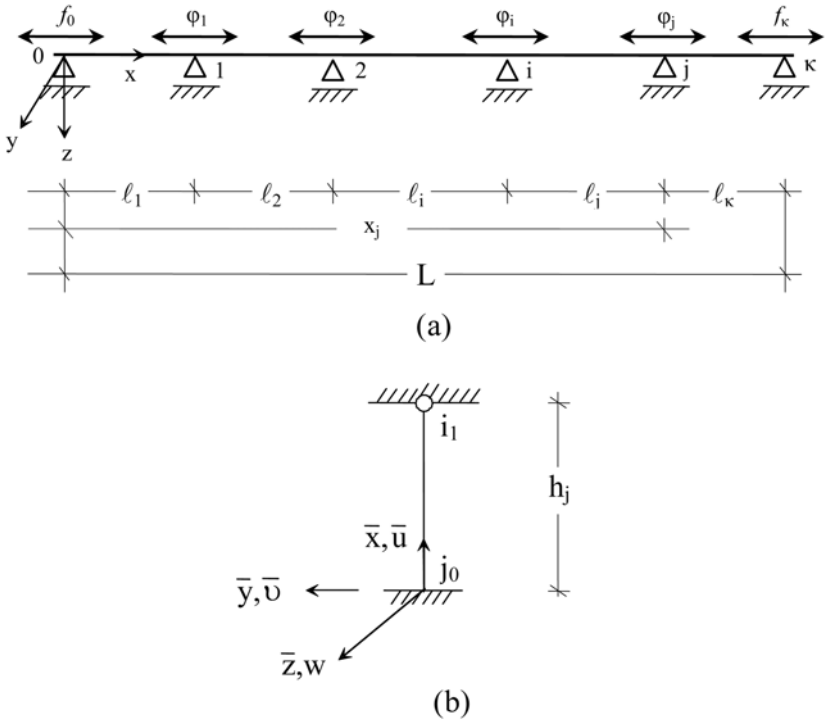

Fig. 2 Model of the system considered (a) entire bridge-deck beam, (b) pylon beam-column

c. We assume that the top of the i^{th} pylon moves according to the time function $\varphi_i(t)$, which has to be determined.
d. The system considered can be analyzed by combining the bridge-deck continuous beam shown in Fig. 2a, with known eigenshapes U_n, X_n and eigenfrequencies ω_n, and the single pylon beam-column systems shown in Fig. 2(b), with also known eigenshapes $\bar{X}_n$ and eigenfrequencies $\bar{\omega}_n$.
e. The time functions f_i representing the displacement of the pylon bases are known, while the functions φ_i representing the movement of the pylon tops will be determined.
f. The axial motion of the continuous beam-deck system is not affected by the bending and torsional motions (uncoupled system).

All geometrical and material properties of the pylons will be outlined within the text. The "influence functions" $g_i(x)$ of the bridge with unit displacement at support i are known, and so are $g_i(x) = x/\ell_i$ for span i and $g_{i+1}(x) = (\ell_{i+1} - x)/\ell_{i+1}$ for span $i+1$.

3. Analytical model

3.1 Governing equations of motion

Neglecting the effect of damping, the equations of motion of the beam for axial and bending vibration are as follows

$$EAu''(x,t) - m\ddot{u}(x,t) = 0$$
$$EJ_y w''''(x,t) + P(x,t)w''(x,t) + m\ddot{w}(x,t) = 0 \quad (1)$$

where $P(x,t)$ is the axial force caused by the axial motion of the beam, EA is the axial stiffness, EJ_y is the bending stiffness and m is the mass per unit length of the beam.

3.2 The axial motion of the beam

For the $(j-1)-j$ span of the beam, the total elongation or shortening will be $\Delta\ell_{(j-1)j} = \varphi_j - \varphi_{j-1}$, and the corresponding axial force P_j at node j is

$$P_j = \frac{EA}{\ell_j} \cdot (\varphi_j - \varphi_{j-1}) \quad (2)$$

where ℓ_j is the length of the span j. At the top of pylon j, the shear force V_j developed is

$$V_j = \frac{3E\bar{J}_{yj}}{h_j^3} \cdot (\varphi_j - f_j) \quad (3)$$

where $E\bar{J}_{yj}$ is the bending stiffness and h_j the height of the pylon j, respectively. Equilibrium of the forces acting at the j^{th} node (Fig. 3) gives

$$-P_j - V_j + P_{j+1} = 0 \quad (4a)$$

By using Eqs. (2) and (3), the preceding relation (4a) becomes

$$-\alpha_j(\varphi_j - \varphi_{j-1}) - \beta_j(\varphi_j - f_j) + \alpha_{j+1}(\varphi_{j+1} - \varphi_j) = 0 \quad (4b)$$

or finally, to the following linear system (for $j = 1$ to κ)

$$\alpha_j\varphi_{j-1} - (\alpha_j + \alpha_{j+1} + \beta_j)\varphi_j + \alpha_{j+1}\varphi_{j+1} = -\beta_j f_j \quad (4c)$$

where the coefficients α_j and β_j are given by

$$\alpha_j = \frac{EA}{\ell_j}, \beta_j = \frac{3E\bar{J}_y}{h_j^3} \quad (4d)$$

Hence, the displacements φ_j ($j = 1$ to κ) at the pylon tops can be determined by solving the following set of linear equations (4c), which in matrix form can be written as follows

$$\begin{vmatrix} -(\alpha_1+\alpha_2+\beta_1) & \alpha_2 & 0 & \cdots \\ \alpha_2 & -(\alpha_2+\alpha_3+\beta_2) & \alpha_3 & \cdots \\ \cdots & \cdots & \cdots & \cdots \\ \cdots & \alpha_{\kappa-2} & -(\alpha_{\kappa-2}+\alpha_{\kappa-1}+\beta_{\kappa-2}) & \alpha_{\kappa-2} \\ \cdots & 0 & \alpha_{\kappa-1} & -(\alpha_{\kappa-1}+\alpha_\kappa+\beta_{\kappa-1}) \end{vmatrix} \begin{vmatrix} \varphi_1 \\ \varphi_2 \\ \vdots \\ \varphi_{\kappa-2} \\ \varphi_{\kappa-1} \end{vmatrix} = \begin{vmatrix} \beta_1 f_1 - \alpha_1 f_o \\ \beta_2 f_2 \\ \vdots \\ \beta_{\kappa-2} f_{\kappa-2} \\ \beta_{\kappa-1} f_{\kappa-1} - \alpha_\kappa f_\kappa \end{vmatrix} \quad (5)$$

Let us consider now the beam that represents the bridge-deck system as shown in Fig. 2(a). The total axial displacement of the beam is

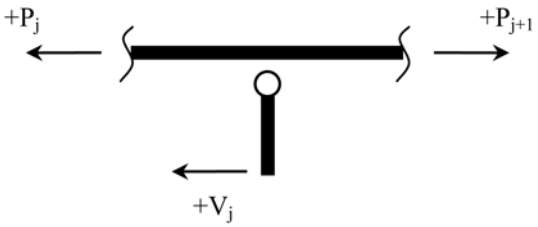

Fig. 3 Equilibrium at node *j*

$$u(x,t) = u_{st}(x,t) + u_o(x,t),$$

or

$$u(x,t) = \sum_{j=1}^{\kappa-1} g_j(x)\varphi_j(t) + g_o(x)f_o(t) + g_\kappa(x)f_\kappa(t) + u_o(x,t) \tag{6}$$

where u_{st} is the displacement of the beam as a solid, u_o is the elastic deformation, g_j are the influence functions for unit axial displacement of the j^{th} support, and $\varphi_j(t)$ the functions representing the movement of the pylon tops, given by the solution of the linear equations of Eq. (5).

The equation of axial motion of the deck beam is the first of Eqs (1). By substituting $u(x, t)$ from Eq. (6) into this equation, we obtain

$$EAu_o''(x,t) - m\ddot{u}_o(x,t) = m\ddot{u}_{st}(x,t) = m\sum_{j=1}^{\kappa-1} g_j(x)\ddot{\varphi}_j(t) + mg_o(x)\ddot{f}_o(t) + mg_\kappa(x)\ddot{f}_\kappa(t) \tag{7}$$

We are searching for a solution with the form

$$u_o(x,t) = \sum_n U_n(x)\cdot T_n(t) \tag{8}$$

where $U_n(x)$ are the shape functions of the beam in axial vibrations and $T_n(t)$ are functions of t, which are to be determined. Substituting Eq. (8) into Eq. (7) yields

$$EA\sum_n U_n'' T_n - m\sum_n U_n \ddot{T}_n = m\sum_{j=1}^{\beta\kappa-1} g_j\varphi_j + mg_o\ddot{f}_o + mg_\kappa\ddot{f}_\kappa \tag{9a}$$

Since U_n satisfies the equation of free motion $EAU'' + m\omega_{\alpha n}^2 U_n = 0$, Eq. (9a) will take the following form

$$-m\sum_n \omega_{\alpha n}^2 U_n T_n - m\sum_n U_n \ddot{T}_n = m\left(\sum_{j=1}^{\kappa-1} g_j\ddot{\varphi}_j + g_o\ddot{f}_o + g_\kappa\ddot{f}_\kappa\right) \tag{9b}$$

Accordingly

$$\ddot{T}_n + \omega_{\alpha n}^2 T_n = -\sum_{j=1}^{\kappa-1} A_{jn}\ddot{\varphi}_j(t) - A_{on}\ddot{f}_o(t) - A_{\kappa n}\ddot{f}_\kappa(t) \tag{10a}$$

where

$$A_{jn} = \frac{\int_0^L g_j(x)U_n(x)dx}{\int_0^L U_n^2(x)dx}, A_{on} = \frac{\int_0^L g_o(x)U_n(x)dx}{\int_0^L U_n^2(x)dx}, A_{\kappa n} = \frac{\int_0^L g_\kappa(x)U_n(x)dx}{\int_0^L U_n^2(x)dx} \tag{10b}$$

The solution of Eq. (10a) is given by the Duhamel's integral and is

$$T_n = -\sum_{j=1}^{\kappa-1}\left(\frac{A_{jn}}{\omega_{\alpha n}}\int_0^t \ddot{\varphi}_j(\tau)\cdot\sin\omega_{\alpha n}(t-\tau)d\tau\right) - \int_0^t\left(\frac{A_{on}}{\omega_{\alpha n}}\ddot{f}_o(\tau) + \frac{A_{\kappa n}}{\omega_{\alpha n}}\ddot{f}_\kappa(\tau)\right)\sin\omega_{\alpha n}(t-\tau)d\tau \tag{11}$$

3.3 The flexural motion of the beam

The axial force P developed on the beam is

$$P(x,t) = EAu'(x,t) \tag{12a}$$

The reactions of the supports, acting on the deck with eccentricity e_z, will produce moments M at positions $x = x_j$ as follows

$$M_o = -P_1 e_z = -\frac{EA}{\ell_1}(\varphi_1 - f_o)e_z$$

$$M_j = -V_j e_z = -\frac{3E\bar{I}_y}{h_j^3}(\varphi_j - f_j)e_z \tag{12b}$$

$$M_\kappa = -P_\kappa e_z = -\frac{EA}{\ell_\kappa}(f_\kappa - \varphi_{\kappa-1})e_z$$

Substituting Eqs. (12a) and (12b) into the second of Eq. (1), we obtain the following equation of motion for the beam

$$\begin{aligned} EI_y w''''(x,t) + m\ddot{w}(x,t) &= -EAu'(x,t)w''(x,t) - \frac{EA}{\ell_1}(\varphi_1 - f_o)e_z\delta'(x-0) \\ &-\sum_{j=1}^{\kappa}\frac{3E\bar{I}_y}{h_j^3}(\varphi_j - f_j)e_z\delta'(x-x_j) - \frac{EA}{\ell_\kappa}(f_\kappa - \varphi_{\kappa-1})e_z\delta'(x-x_\kappa) \end{aligned} \tag{13a}$$

where δ is the Dirac function and

$$u'(x,t) = \sum_{j=1}^{\kappa} g'_j(x)\varphi_j(t) + g'_o(x)f_o(t) + g'_\kappa(x)f_\kappa(t) + \sum_n U'_n(x)T_n(t) \tag{13b}$$

Since the bending moment M depends mainly on the eccentricity of the support's reaction, one can neglect the first term on the right-hand side of Eq. (13a). The time function obtained by solution of

the preceding equation using the above procedure can be regarded as the first approximation for a more accurate study of the bending motion (Krasnov *et al*. 1971).

Thus, the first step is to solve for the following equation

$$EI_y w''''(x,t) + m\ddot{w}(x,t) = \frac{EA}{\ell_1}(\varphi_1 - f_o)e_z\delta'(x-0) - \sum_{j=1}^{\kappa}\frac{3E\bar{I}_y}{h_j^3}(\varphi_j - f_j)e_z\delta'(x-x_j) - \frac{EA}{\ell_\kappa}(f_\kappa - \varphi_{\kappa-1})e_z\delta'(x-x_\kappa) \tag{14}$$

We are searching for a solution of the form

$$w(x,t) = \sum_k X_k(x)\Phi_k(t) \tag{15}$$

where $X_k(x)$ are the shape functions of the beam and $\Phi_k(t)$ are the unknown time functions to be determined. Substituting Eq. (15) into Eq. (14), multiplying by X_m, integrating the outcome from 0 to L, and using the orthogonality conditions (Lovitt 1924), we can arrive at the following equation for the m^{th} time function

$$\ddot{\Phi}_m + \omega_m^2\Phi_m = -\frac{e_z}{m\int_0^L X_m^2 dx}\left\{EA\int_0^L \frac{\Phi_1 - f_o}{\ell_1}X_m(x)\delta'(x-0)dx + 3E\bar{I}_y\int_0^L\sum_{j=1}^{\kappa-1}\frac{\Phi_j - f_j}{h_j^3}X_m(x)\delta'(x-x_j)dx\right.$$

$$\left. + EA\int_0^L \frac{f_\kappa - \varphi_{\kappa-1}}{\ell_\kappa}X_m(x)\delta'(x-x_\kappa)dx\right\}$$

or

$$\ddot{\Phi}_m + \omega_m^2\Phi_m = \frac{e_z}{m\int_0^L X_m^2 dx}\left\{EA\frac{\varphi_1 - f_o}{\ell_1}X'_m(0) + 3E\bar{I}_y\sum_{j=1}^{\kappa-1}\frac{\varphi_j - f_j}{h_j^3}X'_m(x_j) + EA\frac{f_\kappa - \varphi_{\kappa-1}}{\ell_\kappa}X'_m(x_\kappa)\right\} \tag{16}$$

The solution of the above equation is given by Duhamel's integral as follows

$$\ddot{\Phi}_m = \frac{e_z}{m\omega_m\int_0^L X_m^2 dx}\left\{EAX'_m(0)\int_0^t \frac{\varphi_1(\tau) - f_o(\tau)}{\ell_1}\sin[\omega_m(t-\tau)]d\tau + 3E\bar{I}_y X'_m(x_j)\int_0^t\sum_{j=1}^{\kappa-1}\frac{\varphi_j(\tau) - f_j(\tau)}{h_j^3}\right.$$

$$\left.\sin[\omega_m(t-\tau)]d\tau + EAX'_m(x_\kappa)\int_0^t \frac{f_\kappa(\tau) - \varphi_{\kappa-1}(\tau)}{\ell_\kappa}\sin[\omega_m(t-\tau)]d\tau\right\} \tag{17}$$

The second step is to introduce the time function Φ_m (t) obtained above into the right-hand side of Eq. (13a), resulting in

$$EI_y w''''(x,t) + m\ddot{w}(x,t) = -EAu'(x,t)\sum_n X''_n(x)\Phi_n(t) - \frac{EA}{\ell_1}(\varphi_1 - f_o)e_z\delta'(x-0)$$

$$-\sum_{j=1}^{\kappa}\frac{3E\bar{I}_y}{h_j^3}(\varphi_j-f_j)e_z\delta'(x-x_j)-\frac{EA}{\ell_\kappa}(f_\kappa-\varphi_{\kappa-1})e_z\delta'(x-x_\kappa) \tag{18}$$

Here, we are searching for a solution of the form

$$w(x,t)=\sum_k X_k(x)\bar{\Phi}_k(t) \tag{19}$$

where $\bar{\Phi}_k(t)$ is the second step (new) time function to be determined.

Following a procedure similar to the above for determination of Φ_m, we can arrive at the following differential equation

$$\ddot{\bar{\Phi}}_m+\omega_m^2\bar{\Phi}_m=-\frac{EA}{m\omega_m\int_0^L X_m^2dx}\int_0^L u'(x,t)\Big(\sum_n X''_n(x)\Phi_n(t)\Big)X_m(x)dx$$
$$+\frac{e_z}{m\int_0^L X_m^2dx}\left\{EA\frac{\Phi_1-f_o}{\ell_1}X'_m(0)+3E\bar{I}_y\sum_{j=1}^{\kappa-1}\frac{\Phi_j-f_j}{h_j^3}X'_m(x_j)+EA\frac{f_\kappa-\varphi_{\kappa-1}}{\ell_\kappa}X'_m(x_\kappa)\right\} \tag{20}$$

The solution of Eq. (20) is given by Duhamel's integral as follows

$$\bar{\Phi}_m=-\frac{EA}{m\omega_m\int_0^L X_m^2dx}\int_0^t\left(\int_0^L u'(x,\tau)\Big(\sum_n X''_n(x)\Phi_n(\tau)\Big)X_m(x)dx\right)\sin\omega_m(t-\tau)d\tau$$
$$+\frac{e_z}{m\omega_m\int_0^L X_m^2dx}\left\{EAX'_m(0)\int_0^t\frac{\Phi_1(\tau)-f_o(\tau)}{\ell_1}\sin[\omega_m(t-\tau)]d\tau+3E\bar{I}_yX'_m(x_j)\int_0^t\sum_{j=1}^{\kappa-1}\frac{\varphi_j(\tau)-f_j(\tau)}{h_j^3}\sin[\omega_m(t-\tau)]d\tau\right.$$
$$\left.+EAX'_m(x_\kappa)\right. \tag{21}$$

4. Numerical results and discussion

In this section, we shall apply the above results to the following three typical cases. The first case refers to a single-span bridge with supports moving non-synchronously. The second case refers to a two-span bridge whose middle support lies on a cantilever-type pier with height h_1, while all the supports are moving synchronously. In this second case, we shall study the influence of the pier's height on the dynamic behavior of the bridge. Finally, in the third case, a three-span bridge on piers of different heights will be studied.

We prefix some basic principles regarding the supports' movement. We assume that the supports 0 and j of a bridge are moving non-synchronously according to the following expressions

$$f_o=a\cdot e^{-bt}\sin\omega_e t$$
$$\text{and}\quad f_j=k_j\cdot a\cdot e^{-bt}\sin(\omega_e t-\rho_j) \tag{22}$$

where, for the cases studied, $a = 0.05$ is the maximum amplitude of the ground movement at the first pier, f_j is the movement at the jth pier, and

$$k_j = -\cos\rho_j + \sqrt{5 \cdot \cos^2 \rho_j - 1} \tag{23}$$

is a coefficient indicating the decrease in ground movement as the distance from the epicenter increases, $b = 0.2$ is a constant expressing the damping of the earthquake, ω_e is the cycle frequency of the harmonic seismic waves taking, in our case, values from 1 to 15, and ρ_j is the phase angle due to the distance L_j between the two supports 0 and j, given by the relation (Zerva 1999)

$$\rho_j = \omega_e \cdot L_j / v \tag{24}$$

where v is the wave propagation velocity. The values of v depend on the ground and are 5.5 km/sec for granite soil and 1.5 km/sec for mud soil.

The aim of this paper is to study the effect of the piers' different heights and movements on the bridge's dynamic behavior, but not on the proposal of expressions for the support movements. As such, the above simplest expressions proposed by Zerva (1990, 1999) for the supports will be used, instead of the complicated ones given in EC 8. In the present study, we will consider two values for ω_e: namely $\omega_e = 3\ \text{sec}^{-1}$, which corresponds to a distant source earthquake, and $\omega_e = 15\ \text{sec}^{-1}$, which corresponds to a near source earthquake.

4.1 The single-span bridge

We consider a single-span bridge made from isotropic and homogeneous material with modulus of elasticity $E = 2.1*10^8\ \text{KN/m}^2$, length $L = 60$ m, mass per unit length $m = 600$ kg/m, moment of inertia $I_y = 0.60\ \text{m}^4$, and cross-sectional area $A = 0.75\ \text{m}^2$. For this bridge, the data listed in Table 1 are valid.

From Figs. 4 and 5, one can observe the influence of various ground qualities on the seismic excitation and its variation relative to the supports distance.

For the axial motion, we can obtain the eigenfrequencies as $\omega_{a1} = 134.132$, $\omega_{a2} = 402.397$, $\omega_{a3} = 670.661\ \text{sec}^{-1}$ and from Eqs. (6), (8), and (11), we obtain the axial deformations $u(x, t)$. From Fig. 6, one can observe the deformations $u(L, t)$ of the right end of the bridge for the case of mid-soil (continuous line) and for the case of mud (dashed line). As can be seen, the difference in the amplitude is generally negligible (~0.5%).

For the flexural motion, the eigenfrequencies can be found as: $\omega_{b1} = 12.563$, $\omega_{b2} = 50.254$, and $\omega_{b3} = 113.071\ \text{sec}^{-1}$. From Eqs. (15) and (21), we can determine the flexural deformations $w(x, t)$. From Fig. 7, one can observe the deformations $w(L/2, t)$ at the midpoint of the bridge for the case of mid-soil (continuous line) and for the case of mud (dashed line). Evidently, the influence of the

Table 1 Properties of soils

	v = 5500 m/sec (granite)		v = 2500 m/sec (mid-soil)		v = 1500 m/sec (mud)	
	ρ	k	ρ	k	ρ	k
$\omega_e = 3$	0.033	0.9992	0.072	0.9961	0.12	0.9892
$\omega_e = 15$	0.164	0.9798	0.36	0.9024	0.60	0.7257

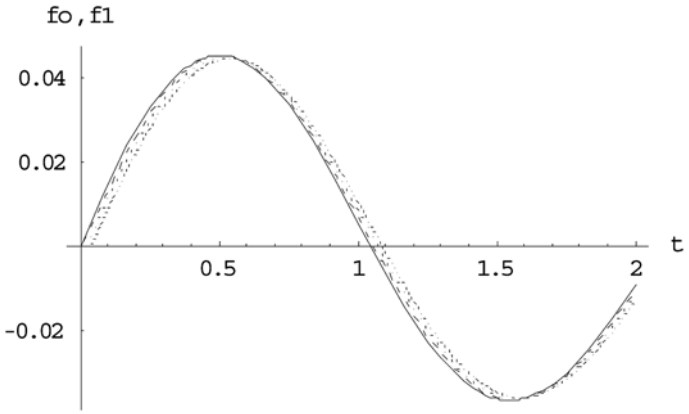

Fig. 4 The seismic excitation of the first support (continuous line), and of the second one for $\omega = 3$ sec^{-1}, $\rho = 0.033$, $k = 0.9992$ (- - -) (granite), $\rho = 0.072$, $k = 0.9961$ (- - -) (middle), $\rho = 0.12$, $k = 0.9892$ (….) (mud)

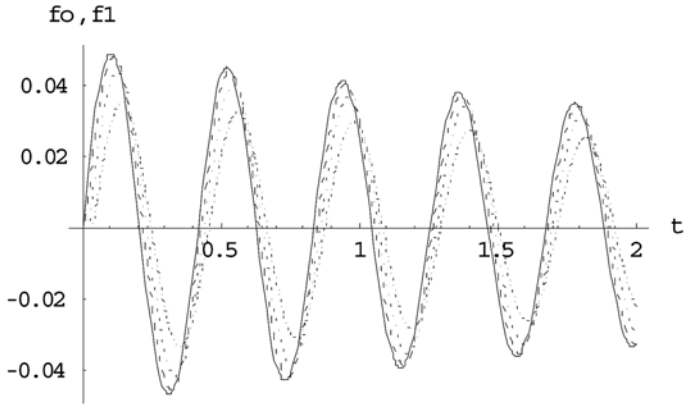

Fig. 5 The seismic excitation of the first support (continuous line), and of the second one for $\omega = 15$ sec^{-1}, $\rho = 0.164$, $k = 0.9798$ (- - -) (granite), $\rho = 0.36$, $k = 0.9024$ (- - -) (middle), $\rho = 0.60$, $k = 0.7257$ (….) (mud)

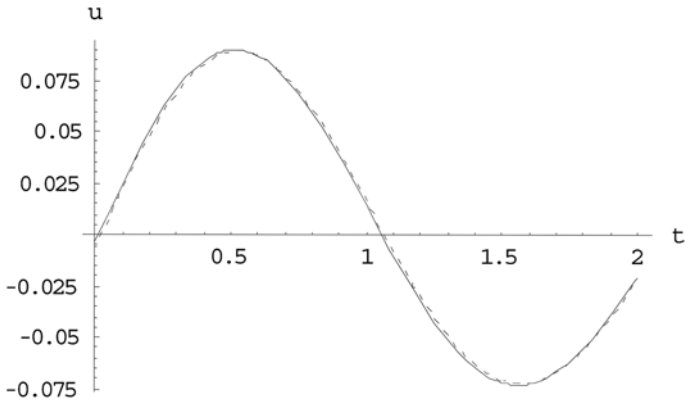

Fig. 6 The axial movement of the right support of the bridge for: mid-soil (___), and mud (_ _ _)

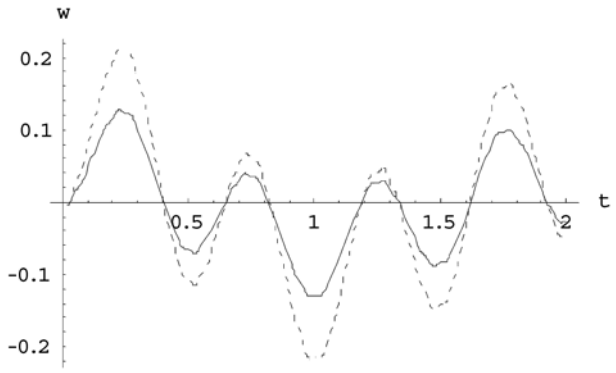

Fig. 7 The flexural movement of the middle point of the bridge for: mid-soil (___), and mud (_ _ _)

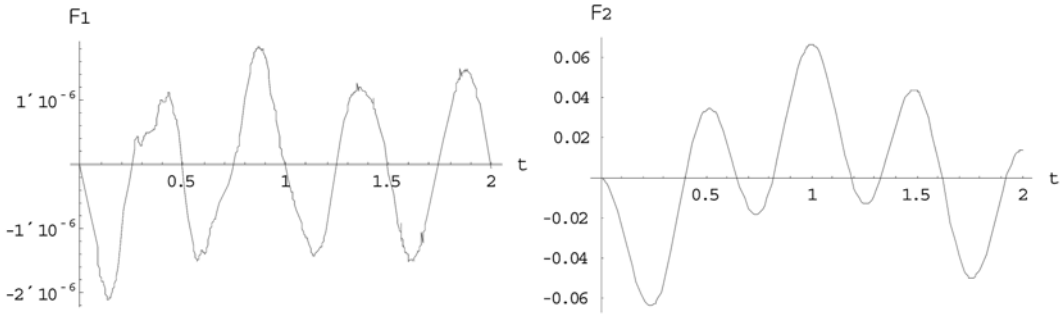

Fig. 8 Contribution of the time functions Φ_1 and Φ_2

ground quality on the amplitude increase is significant, amounting to ~65%. From this example, it is concluded that non-cohesive soils can produce greater relative axial displacements between the two supports and therefore the reactions and corresponding deformations produced are greater than those for cohesive soils.

Now, we can estimate the effect of the two functions Φ_1 and Φ_2, of which the summation constitutes the time function $\overline{\Phi}_m$ in Eq. (21). The plots in Fig. 8 provide a clear picture for the contribution of each of the two functions. We see that function Φ_1 contributes only 0.003% of the total value of function $\overline{\Phi}_m$, and thus it can be neglected.

4.2 The influence of the piers' height (two-span bridge)

We next consider a two-span bridge with a deck having the same properties as those of the bridge in the example of Section 4.1. The span lengths are selected as $L_1 = 60$ m, and $L_2 = 70$ m, and the middle support of the bridge is located on the top of a pylon with height h_1. In addition, we assume that the ground motion (for mid-soil quality) at the left support of the bridge is governed by the relation: $f_o = a \cdot e^{-bt} \sin \omega_e t$, where a, b, ω_e have been given in Section 4.1. Thus, for support 1, we have $k_1 = 0.996$, $\rho_1 = 0.072$, and for support 2 we have $k_2 = 0.983$, $\rho_2 = 0.150$.

In order to study the axial motion, we first find: $\omega_{a1} = 61.907$, $\omega_{a2} = 185.722$, $\omega_{a3} = 309.536$ sec^{-1}. The plots in Fig. 9 show the horizontal movement of the right support of the bridge for supports

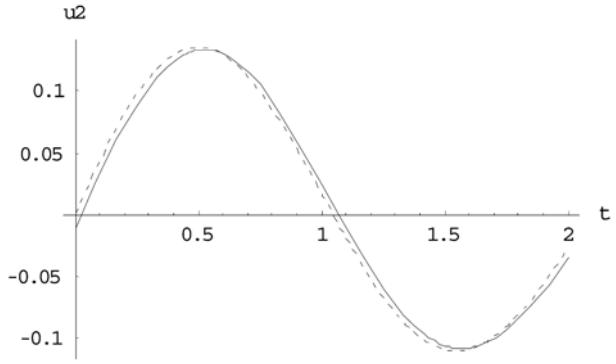

Fig. 9 The movement of the right support for the case of mid-soil (___) and uniform support motion (_ _ _)

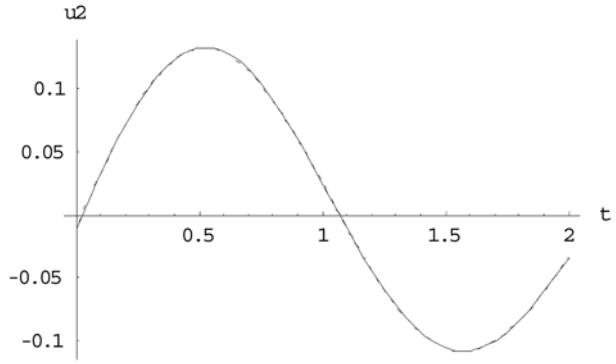

Fig. 10 The movement of the right support for the case of mid-soil for $h1 = 2$ m (___) and $h1 = 20$ m (_ _ _)

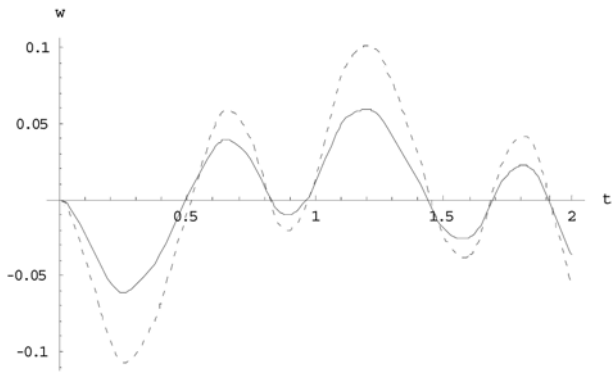

Fig. 11 The deformation of the mid-point of the first span for a mid-soil and mud for pier height $h1 = 10$

with synchronous motion (dashed line) and for supports with non-synchronous motion located on ground with mid-soil quality (continuous line). The maximum difference between the two responses amounts to 4.8%.

The plots in Fig. 10 show the horizontal movement of the right support of the bridge on the

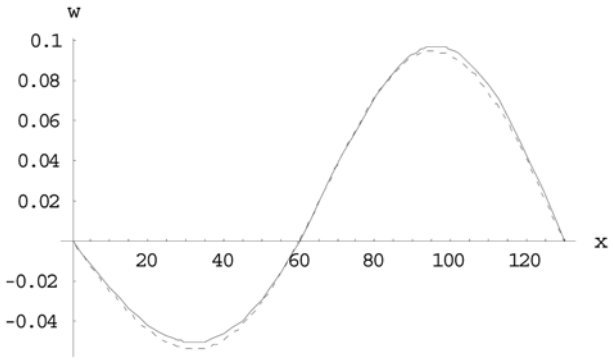

Fig. 12 The deformation of the mid-point of the first span for a mid-soil for $h1 = 2$ m (___), and $h1 = 20$ m (_ _ _)

ground of mid-soil quality for $h_1 = 2$ m and 20 m. The effect of the pier's height is negligible, amounting to 0.05%.

For the study of the flexural motion we find: $\omega_{b1} = 10.347$, $\omega_{b2} = 17.459$, $\omega_{b3} = 40.436$ sec^{-1}. In Fig. 11, one observe that the deformations w_1 ($L_1/2$, t) at the midpoint of the first span of the bridge for the case of mid-soil (continuous line) and for the case of mud (dashed line). The difference of the two responses amounts to ~70%, which is generally large.

From Fig. 12, one can observe the influence of the piers' height on the mid-point of the first span of the bridge for the case of a pier with height $h_1 = 2$ m and that for a pier with height $h_1 = 20$ m. As can be seen, the difference amounts to ~6.50%.

4.3 The influence of the piers' height (three-span bridge)

We consider now a three-span bridge with a deck having the same properties as those of the example in Section 4.1. The span lengths selected are $L_1 = 60$ m, $L_2 = 70$ m, and $L_3 = 60$ m, and the interim supports are assumed to be located on the top of piers with heights h_1 and h_2. In addition, we assume that the motion of the ground (of mid-soil quality or of mud) at the left support of the bridge is governed by the equation: $f_o = a \cdot e^{-bt} \sin \omega_e t$, where a, b, ω_e are given as in Section 4.1. Thus for support 1 we have $k_1 = 0.996$, $\rho_1 = 0.072$, for support 2, we have $k_2 = 0.983$, $\rho_2 = 0.150$, and for support 3, we have $k_3 = 0.960$, $\rho_3 = 0.228$. As for the axial motion, the eigenfrequencies found are: $\omega_{a1} = 42.358$, $\omega_{a2} = 127.073$, $\omega_{a3} = 211.788$ sec^{-1}.

In Fig. 13, the time-history oscillations were plotted of the four supports of the bridge deck supported by piers on mid-soil.

The plots in Fig. 14 show the horizontal movement of the right support of the bridge for supports with synchronous motion (dashed line) and for supports with non-synchronous motion located on ground of mid-soil quality (continuous line). The maximum difference observed amounts to 3.5%. Similar results exist for the middle supports of the bridge with the maximum differences amounting to 2 to 3%.

As for the flexural motion, the eigenfrequencies found are: $\omega_{b1} = 11.010$, $\omega_{b2} = 15.724$, $\omega_{b3} = 20.128$ sec^{-1}. The plots in Fig. 15 show the deformations of the bridge at the instants $t = 1.5$, $t = 2.0$, $t = 2.5$, and $t = 3.0$ sec. We observe that the middle span deforms significantly less than the other two spans.

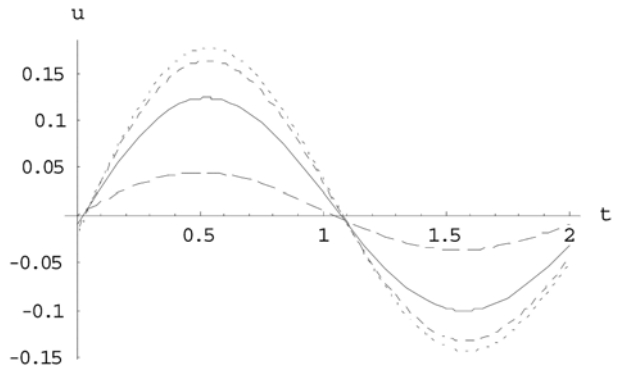

Fig. 13 The deformation of the deck supports of a bridge on mid-soil for $h1 = h2 = 2$ m u_o (__ __), u_1 (___), u_2 (_ _ _), and u_3 (. . . .)

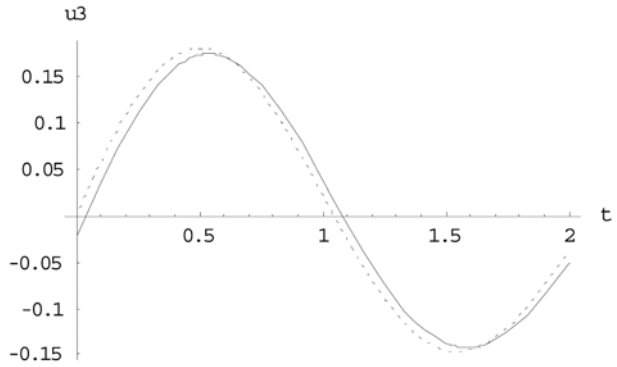

Fig. 14 The movement of the right support for the case of mid-soil (___) and uniform support motion (_ _ _)

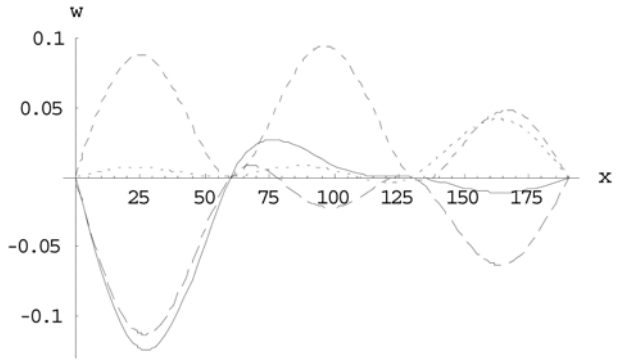

Fig. 15 The deformed bridge deck at $t = 1.50$ (___), $t = 2.00$ (__ __), $t = 2.50$ (_ _ _), and $t = 3.00$ (……)

The three diagrams in Fig. 16 show the oscillations of the middle of the first, second and third span of a bridge on piers of height $h_1 = h_2 = 2$ m, for the grounds of mid-soil and of mud.

Finally, the plots in Fig. 17 show the influence of the piers' height on the flexural motion for different cases of equal (a, b, c, d), and unequal heights (e, f). The influence of the pier's height

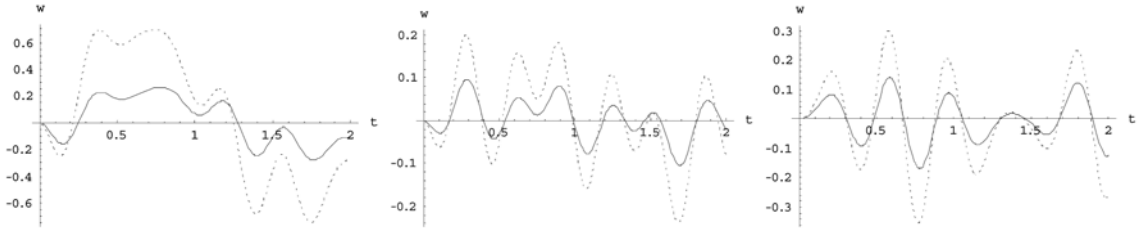

Fig. 16 The flexural oscillations of the mid-point of the first, second, and third span for mid-soil (__) and mud (….)

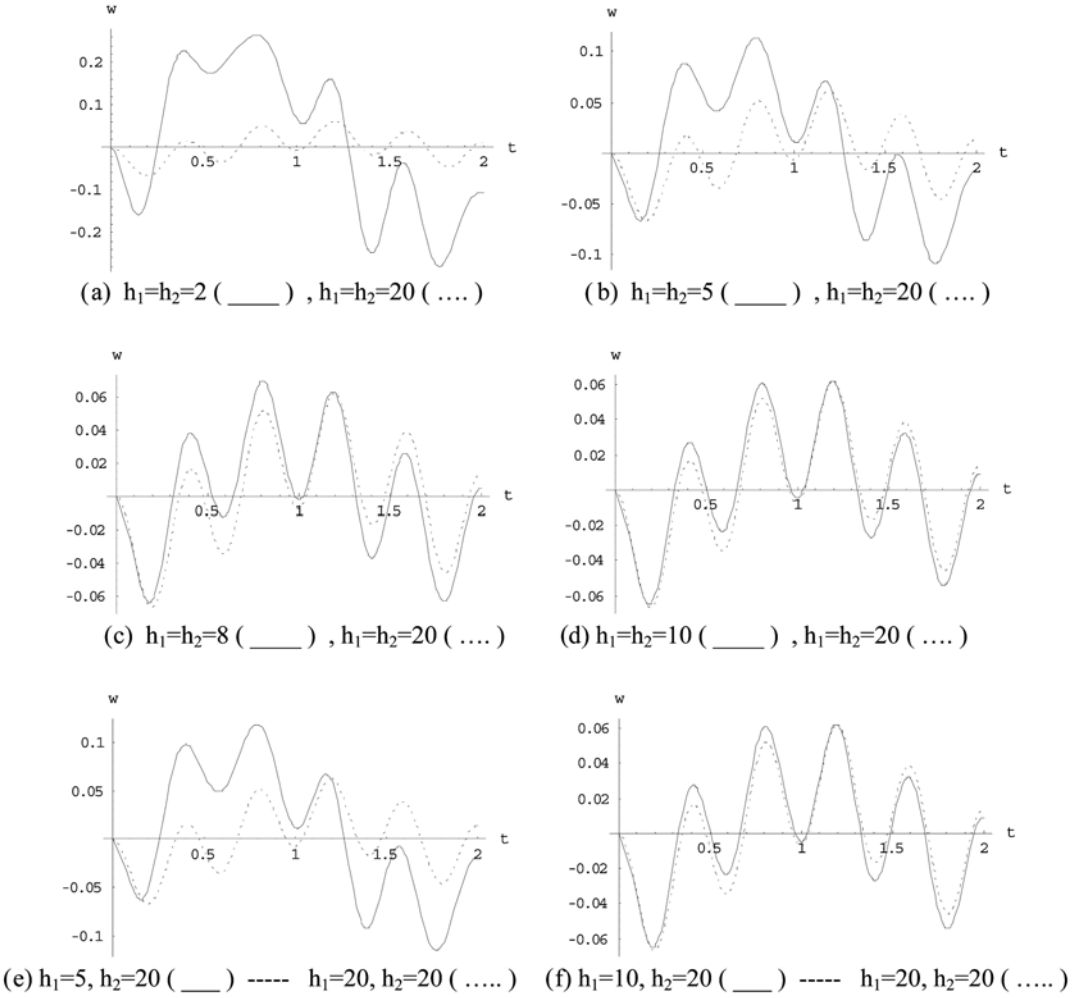

Fig. 17 The influence of the piers' height on the flexural motion for different cases of equal and unequal heights

(short piers produce greater reactions and moments) is generally clear. Even if only one pier is shorter, its influence on the bridge response is significant (see Figs. 17(e) and 17(f)).

5. Conclusions

A simple mathematical model is proposed for studying the dynamic response of a multi-span bridge on piers of different heights under earthquake forces acting in parallel to the bridge axis. From the analyses performed in this study, the following conclusions can be drawn:

a. The properties of the piers (i.e., height and rigidity) strongly affect the oscillations of the bridge.
b. Different ground qualities may produce different movements on the supports, thereby affecting the deformation of the bridge. Such an effect, for the model studied, amounts to about 4%.
c. The increase to the piers' height, for the models studied, causes an increase to the amplitude of deformations in the order of 40% for $J_{pylon} = 0.2$, while for piers with different heights, this amplitude increase drops to 10%.

From the examples studied, it is obvious that following an optimum design for the pylons, one can achieve a satisfactory decrease in the deformations of the bridge and therefore a better overall dynamic behavior of the bridge.

References

Abrahamson, N.A., Schneider, J.F. and Stepp, J.C. (1991), "Empirical spatial coherency functions for application to soil-structures interaction analyses", *Earthq. Spectra,* **7**(1), 41-54.
Betti, R., Abdel-Ghaffar, A.M. and Niazy, A.S. (1993), "Kinematic soil-structure interaction for long-span cable-supported bridges", *Earthq. Eng. Struct. D.,* **22**(5), 415-430.
Bogdanoff, J.L., Goldberg, J.E. and Schiff, A.J. (1965), "The effect of ground transmission time on the response of long structures", *Bull. Seismol. Soc. Am.*, **55**, 627-640.
Eurocode 8-Part 2 (EC8-2) (2002), *Bridges, European Committee for Standardization*, Brussels, ENV 1998-2.
Harichandran, R.S. and Wang, W. (1990), "Response of indeterminate two-span beam to spatially varying seismic excitation", *Earthq. Eng. Struct. D.,* **19**, 173-187.
Krasnov, M., Kiselev, A. and Makarenko, G. (1971), *Problems and exercises in integral equations.* Mir Publishers, Moscow.
Lovitt, W.V. (1924), *Linear Integral Equations*, New York.
Michaltsos, G.T. (2005), *Dynamic problems of Steel Bridges*, (Ed. Symeon), Athens, (in Greek).
Monti, G., Nuti, C. and Pinto, P. (1996), "Nonlinear response of bridges under multisupport excitation", *J. Struct. Eng-ASCE,* **122**(10), 1147-1158.
Nikolaou, A., Mylonakis, G., Gazetas, G. and Tazoh, T. (2001), "Kinematic pile bending during earthquakes: Analysis and measurements", *Geotechnique,* **51**(5), 425-440.
Price, T.E. and Eberhard, M.O. (1998), "Effects of spatially varying ground motions on short bridges", *J. Struct. Eng-ASCE,* **124**(8), 948-955.
Wylie, C.R. (1975), *Advanced Engineering Mathematics,* McGraw-Hill Kogakusha, Ltd., Tokyo.
Zerva, A. (1990), "Response of multi-span beams to spatially incoherent seismic ground motions", *Earthq. Eng. Struct. D.,* **19**(6), 819-832.
Zerva, A. (1999), *Spatial variability of seismic motions recorded over extended ground surface areas*, Wave motion in earthquake engineering. (Eds. kausel, E. and Manolis, G.), MIT Press, Cambridge, Mass.